

Relativistic structured jet

Zakaria Meliani

LUTH

Observatoire de Paris

Outline

- **Motivation**
- **Model**
- **Numerical simulations**
- **Summary**

Two component jet

Origins

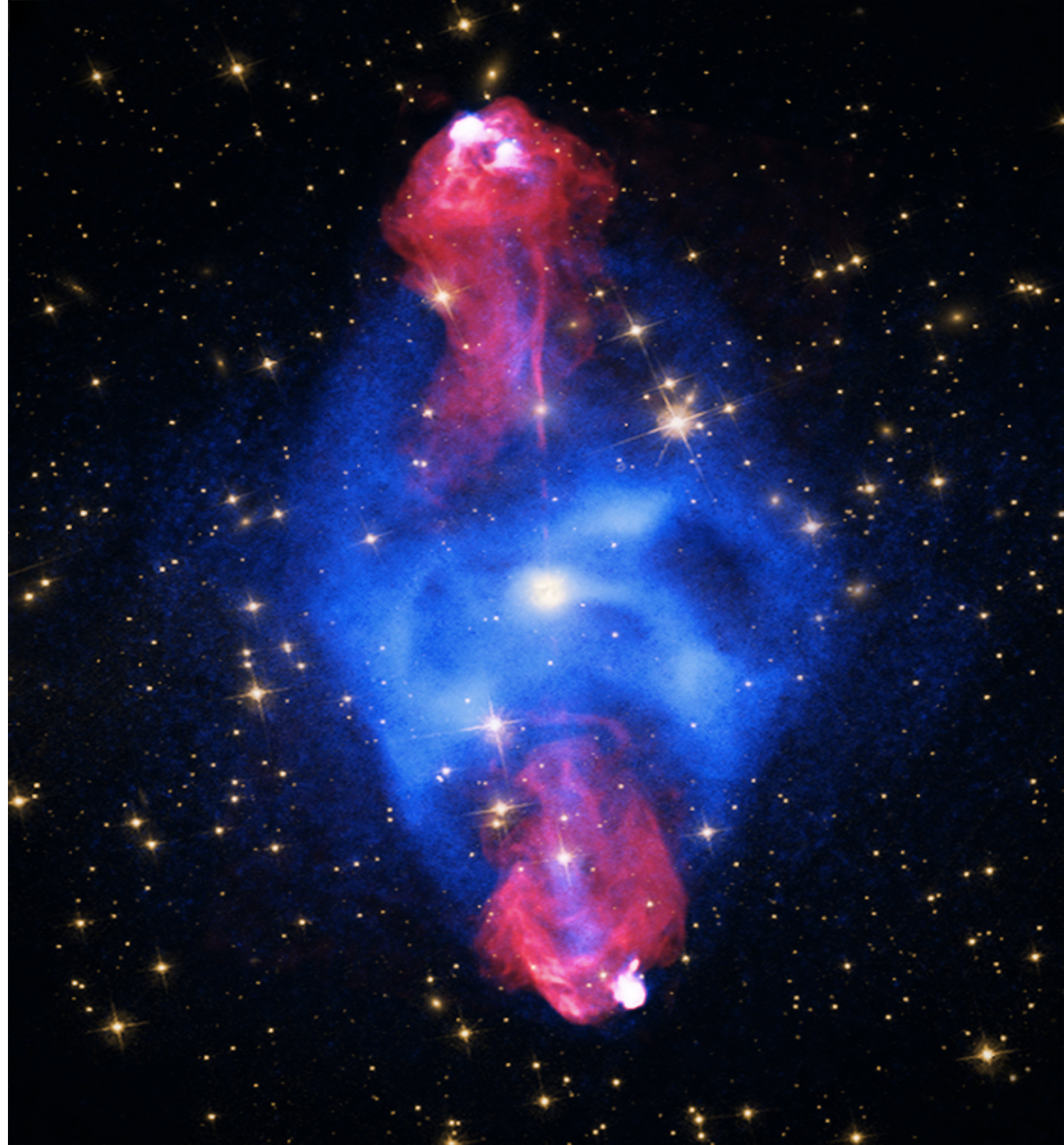
- Jet formation
- Jet propagation

Interactions

- Instabilities
- Shocks
- Current models focus on MHD

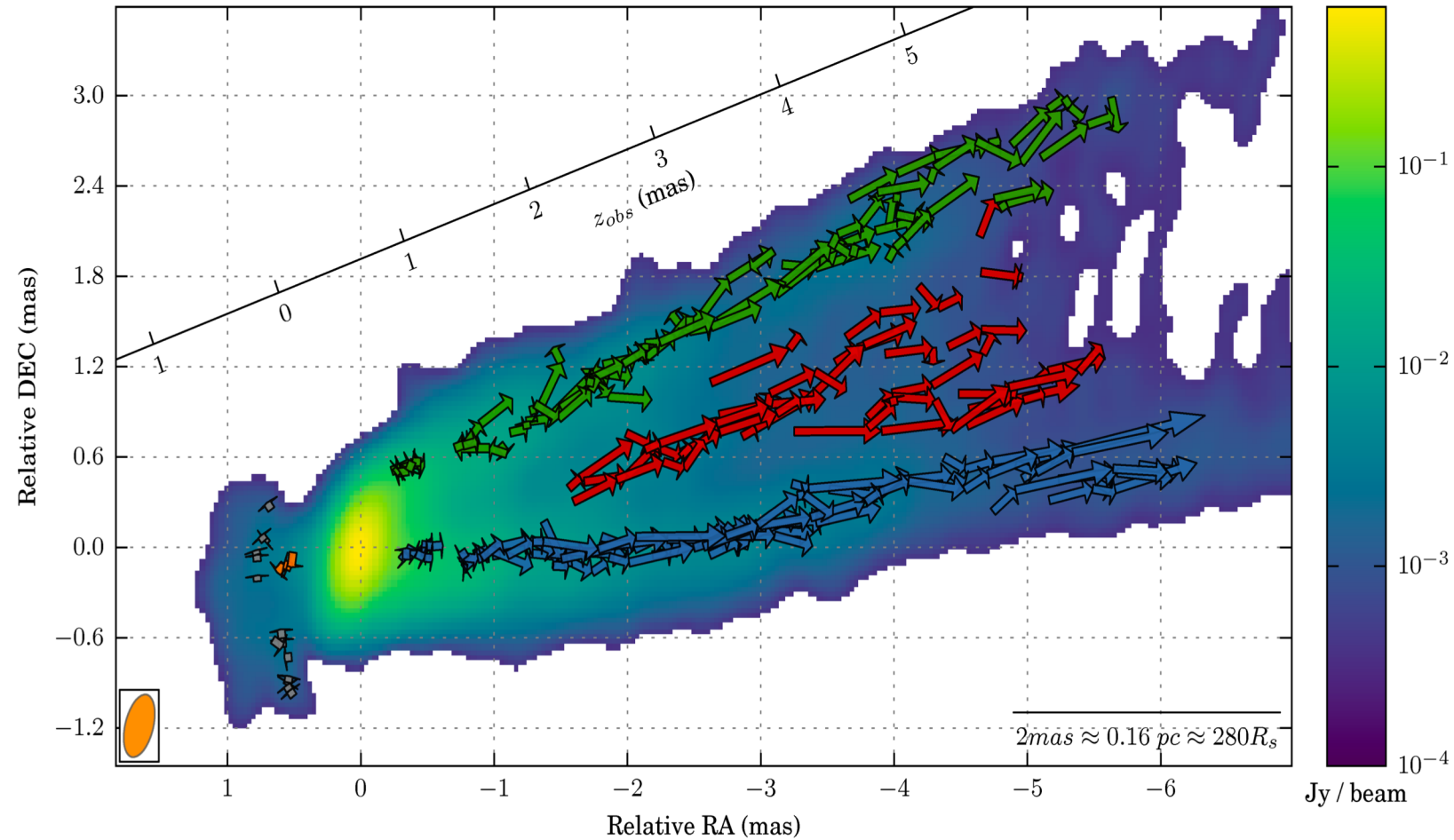
Applications

- AGN classification
- GRB light curves
- Doppler crisis
- gamma ray flares



Structured jet in M87

Edge brightened jet
Central stream and limbs
Evidence for jet rotation

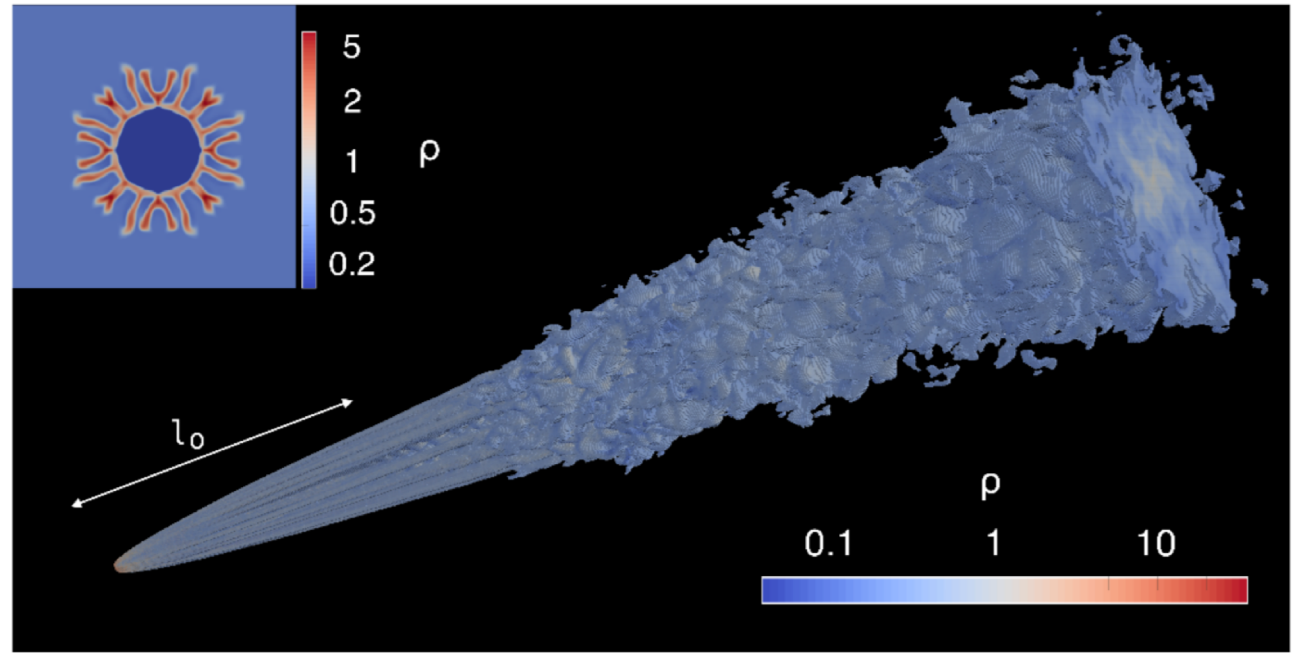


Jet de-collimation

Centrififugal RT instability de-collimation and decelerate the jet

Meliani & Keppens 2007, 2009

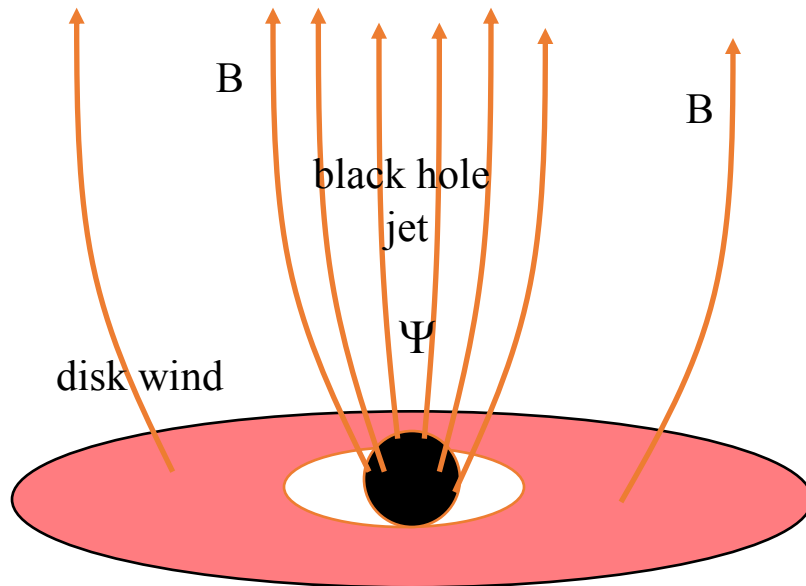
Millas, Keppens & Meliani 2018



Gourgouliatos & Komissarov 2018

Overview – Basic principle de MHD jet production

- Basic MHD mechanism: Blandford (1976); Lovelace (1976)
- Acceleration by rotating black holes (Blandford & Znajek [1977])
- Acceleration by rotating [thin] accretion disks (Blandford & Payne [1982])



- Inertia generates toroidal field and poloidal current
- Acceleration by Lorentz-force $\mathbf{j} \times \mathbf{B} + \rho_e \mathbf{E}$ and thermal force
- Collimation due to tension in the toroidal field

Initial state in a glimpse

Speed profile

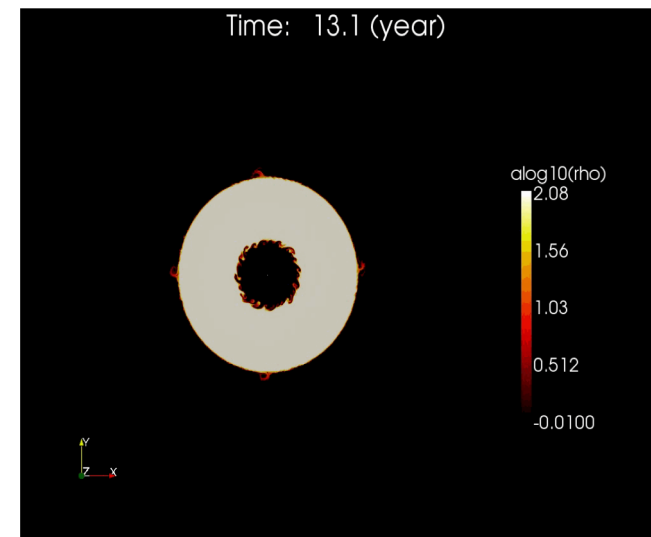
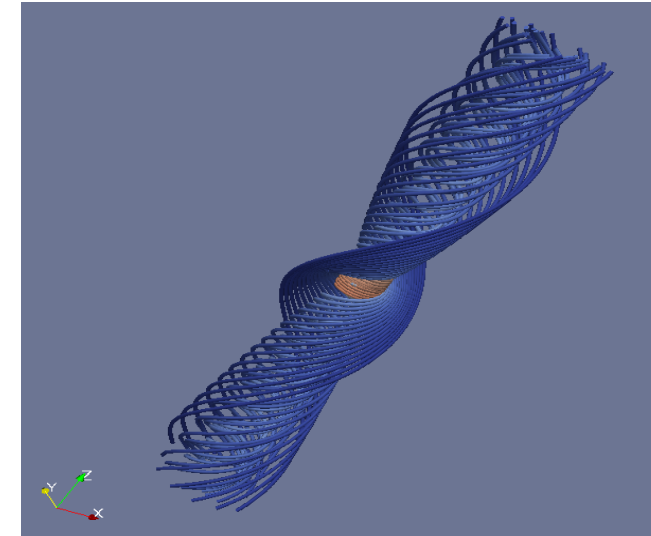
- Lorentz factor **~ 30** (inner jet), **~ 3** (outer jet)
- Approximately constant in each component
- No discontinuity in v_ϕ at the interface but assume differential rotation
- Typical values for AGN jets

Density profile

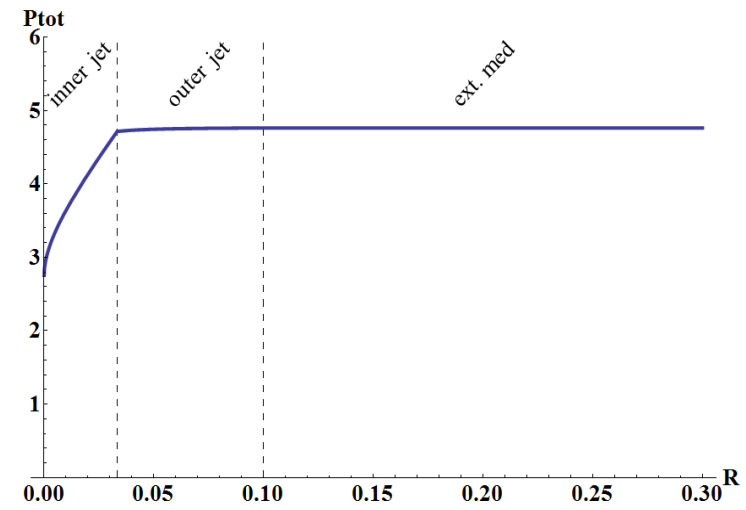
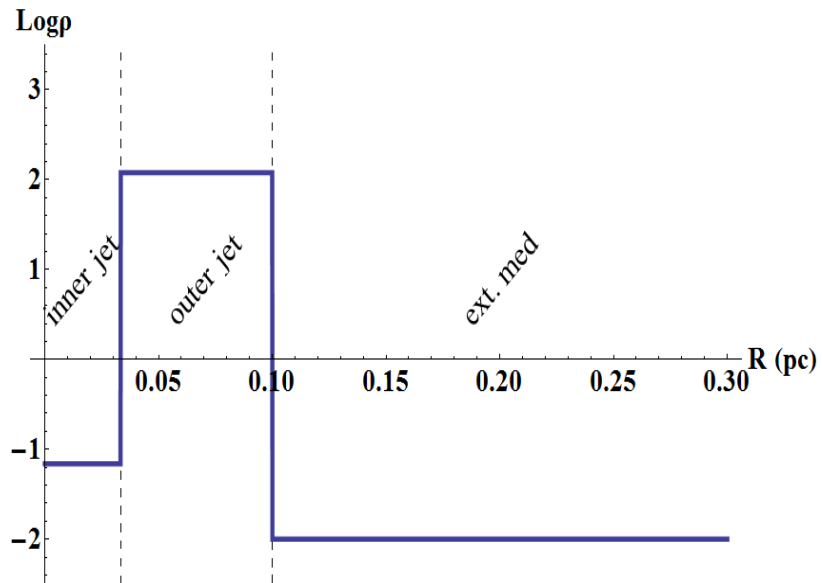
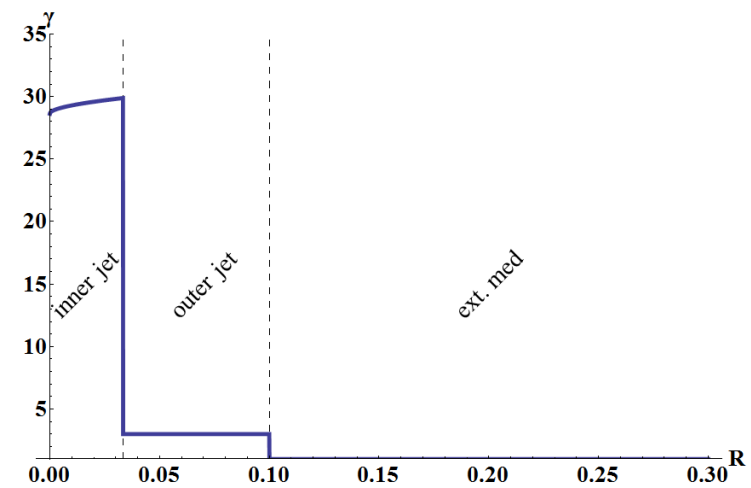
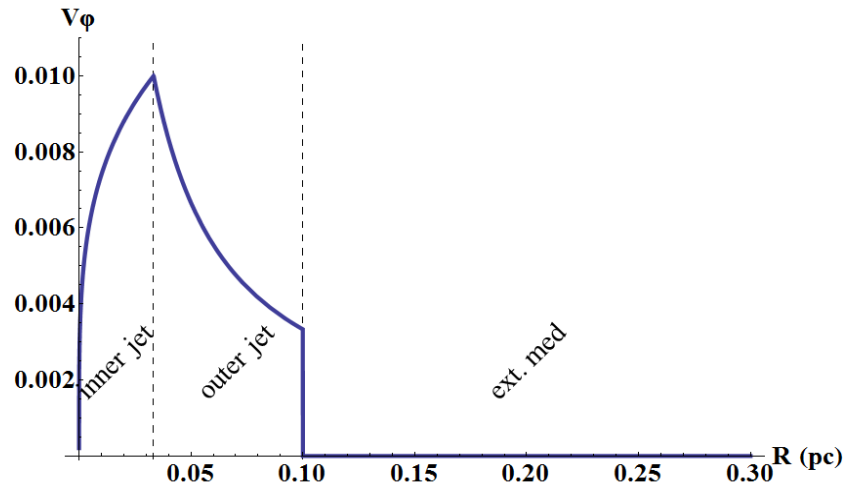
- $$\rho(r) = \begin{cases} 6.92\rho_{ext}, & r \leq r_{in} \\ 119.94 \cdot 10^2 \rho_{ext}, & r_{in} < r < r_{out} \\ \rho_{ext}, & r > r_{out} \end{cases}$$

Assume a polytropic equation of state:

- $\Gamma_{\text{eff,in}} = 4/3$ (hot)
- $\Gamma_{\text{eff,out}} = 5/3$ (cold)



Structured jet model



High energy flux outer jet

Inner wind

1/3 of jet section

Fast $\gamma_z \approx 30$

5% of total energy

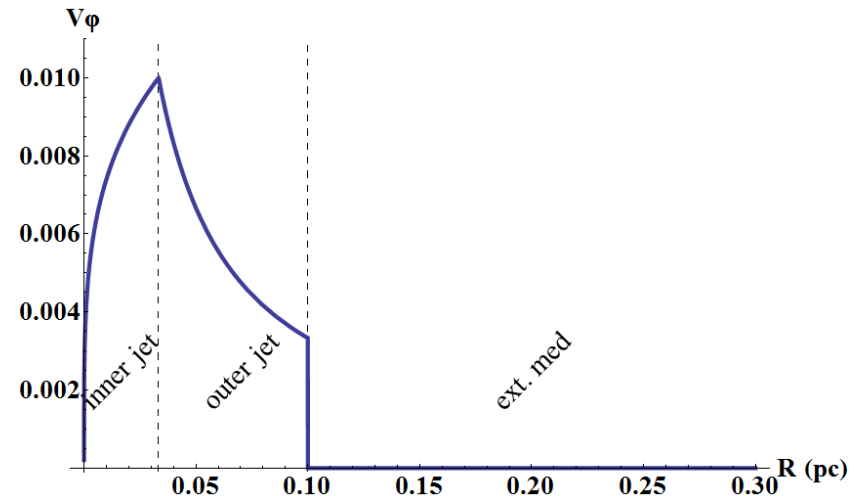
The same amount of angular momentum is extracted by the inner wind and outer jet

Outer jet

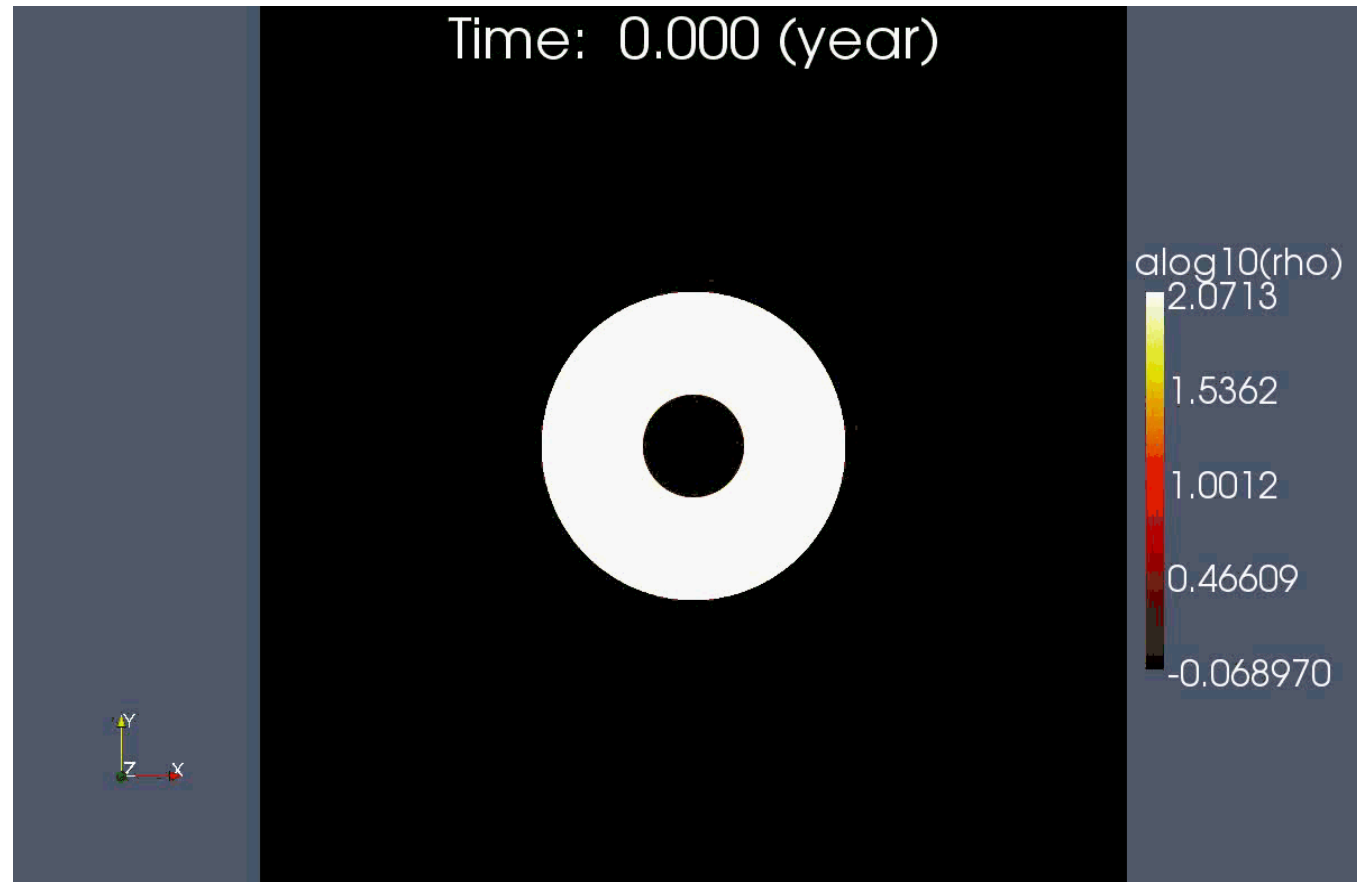
2/3 of jet section

Slow $\gamma_z \approx 3$

95% of total energy



High energy flux outer jet



Logarithm of the comoving frame density

Low energy flux outer jet

Inner wind

1/3 of jet section

Fast $\gamma_z \approx 30$

30% of total energy

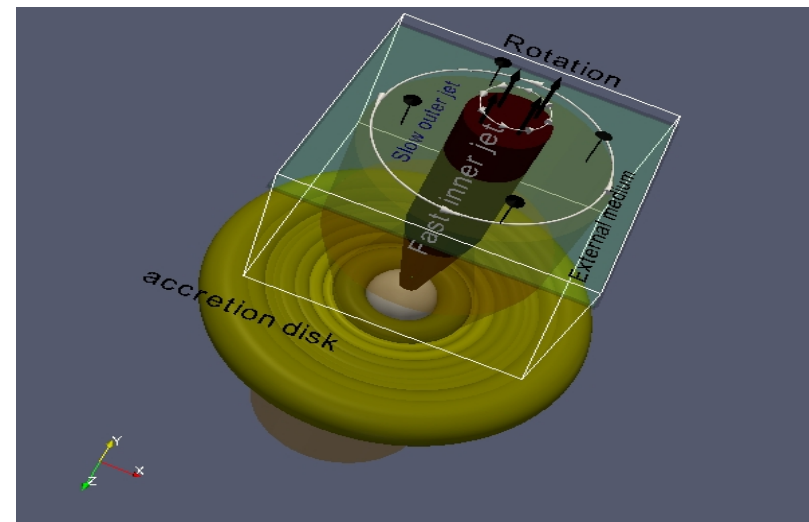
magnetize
(poloidal magnetic field)

Outer jet

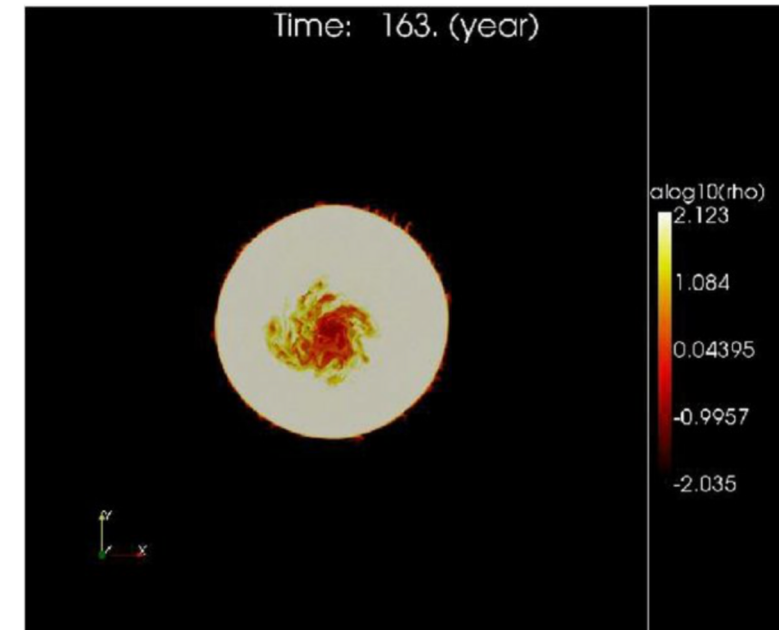
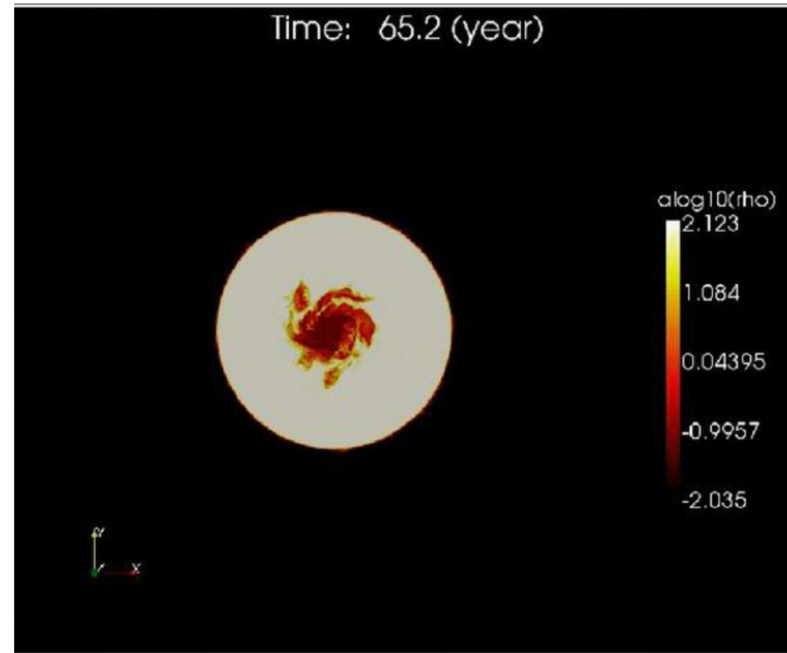
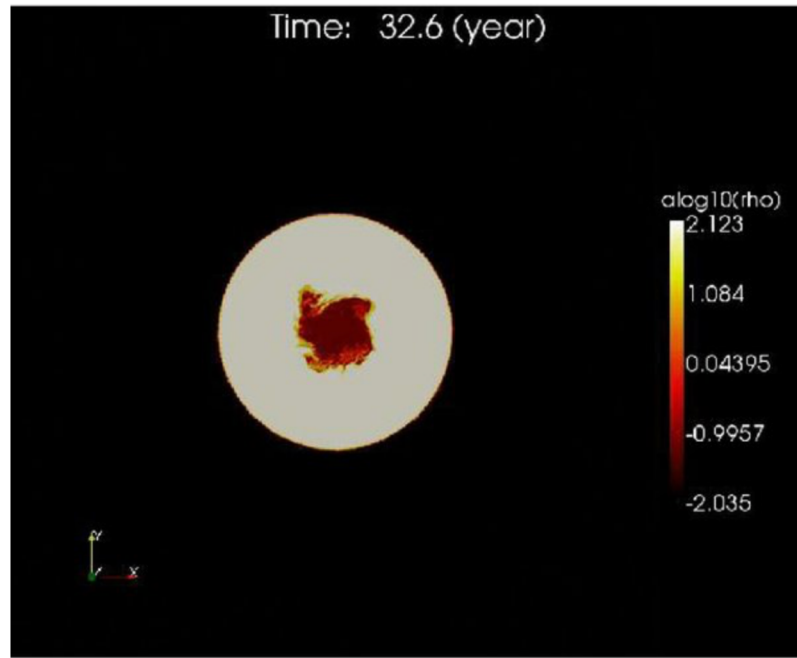
2/3 of jet section

Slow $\gamma_z \approx 3$

70% of total energy

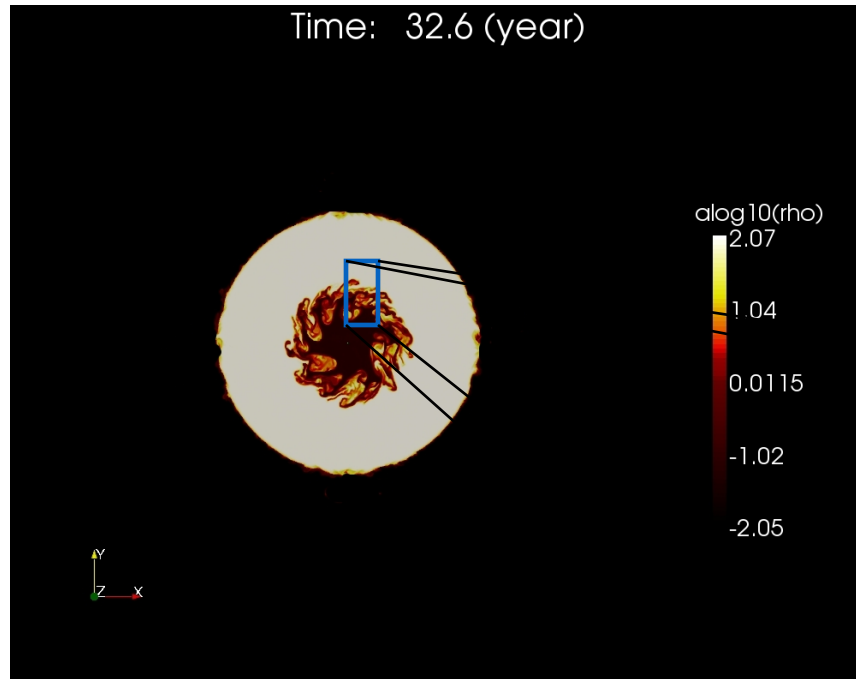


Low energy flux inner flow



Logarithm of the commoving frame density

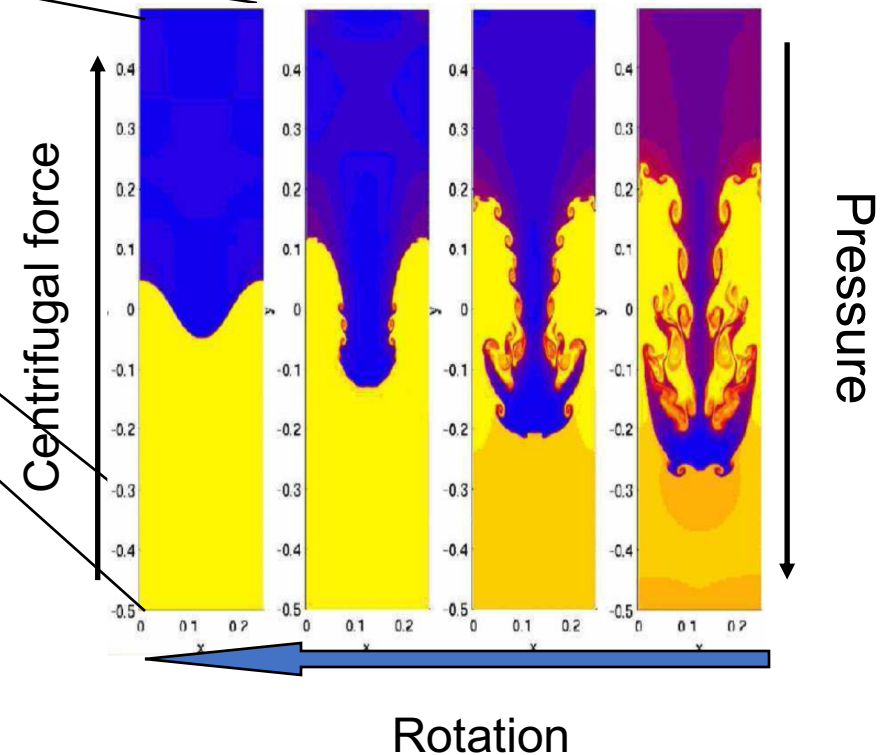
Interface stability



Centrifugal force - pressure equilibrium can be unstable

Angular momentum extraction from the inner jet

Analogous of Rayleigh-Taylor instability



Instability criterion

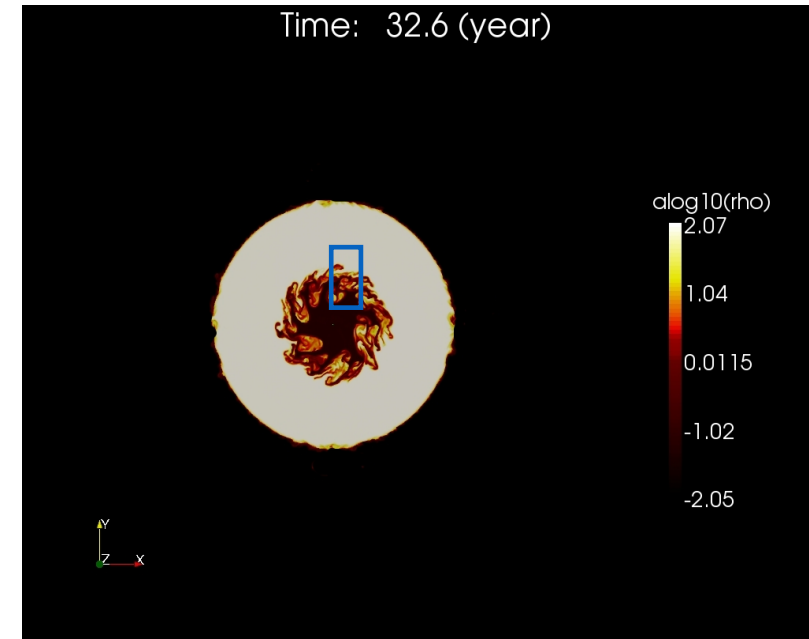
$$\omega \propto k \left[(\gamma^2 h + B_z^2 + \gamma^2 B_\phi^2)_{in} - (\gamma^2 h + B_z^2 + \gamma^2 B_\phi^2)_{out} \right] v^\phi$$

Enthalpy

Toroidal speed

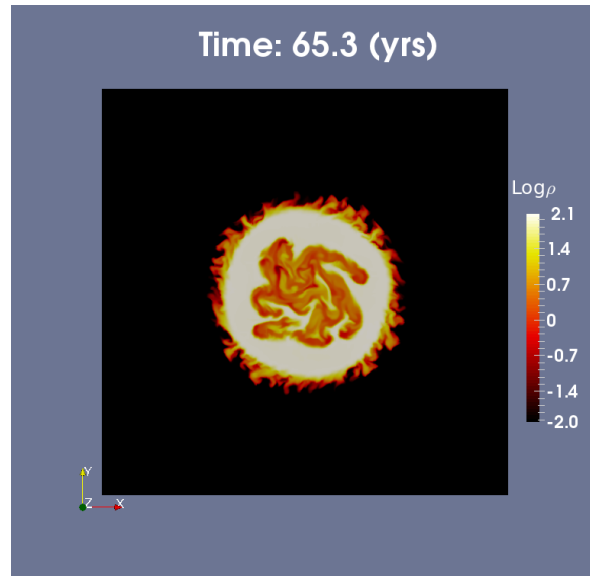
Lorentz factor

Poloidal magnetic field

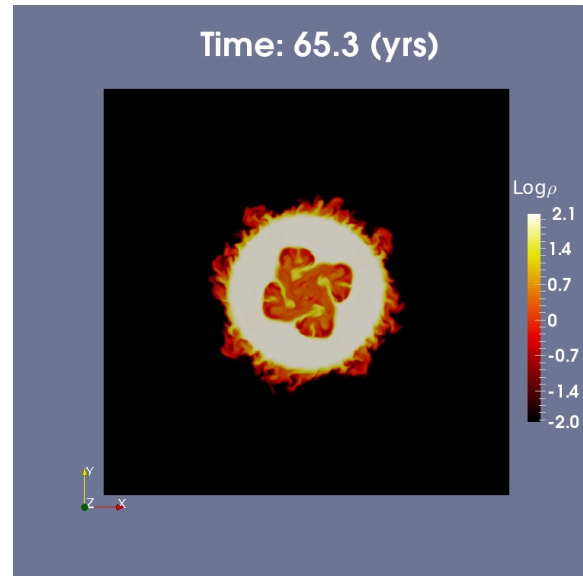


The effects of toroidal magnetic field (phase I)

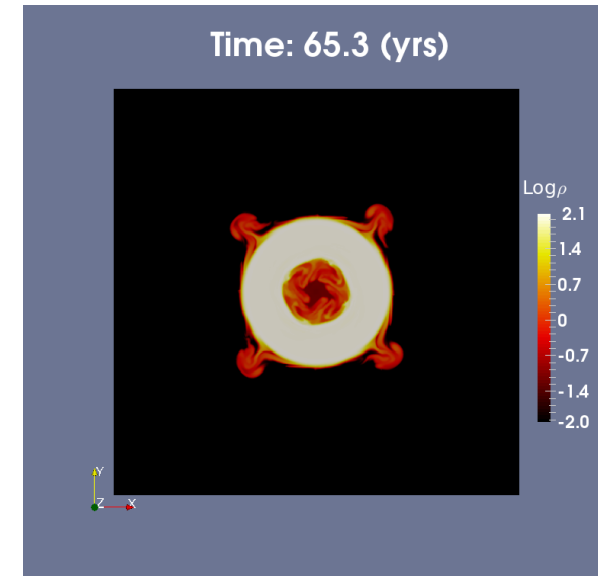
σ



$\sigma = 0.001$



$\sigma = 0.01$

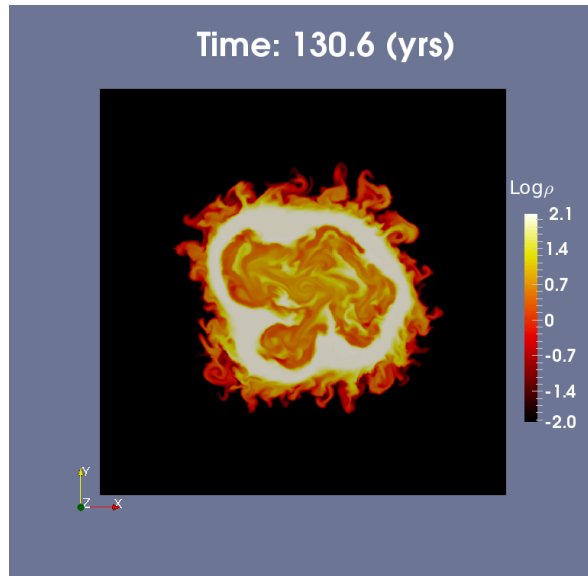


$\sigma = 0.1$

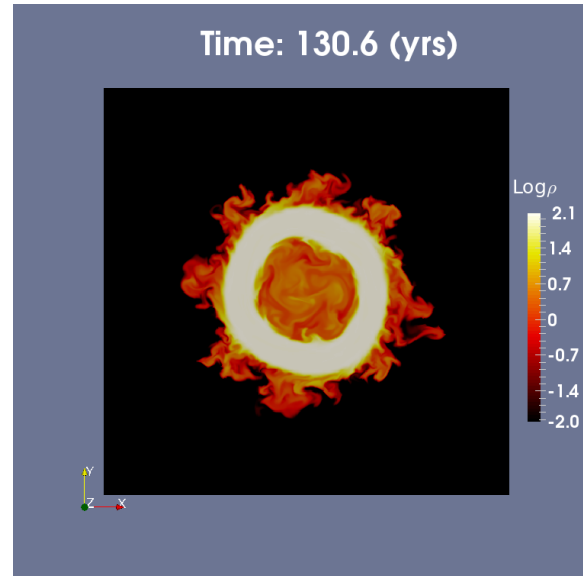
$t = 1$ rotation

The effects of toroidal magnetic field (phase II)

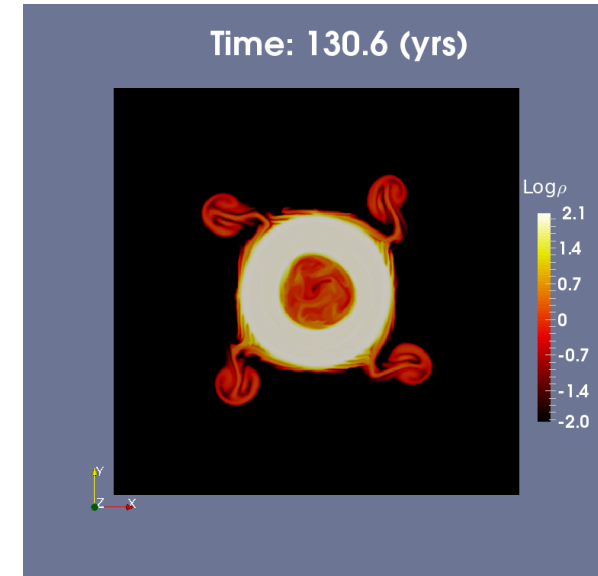
σ



$\sigma = 0.001$



$\sigma = 0.01$

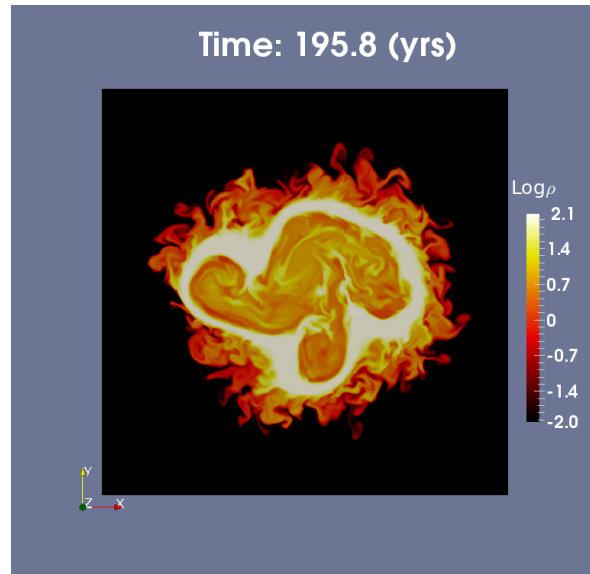


$\sigma = 0.1$

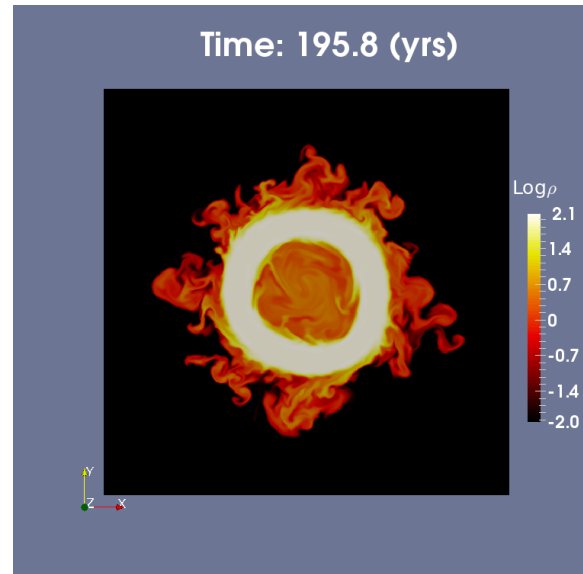
$t = 2$ rotations

The effects of toroidal magnetic field (phase III)

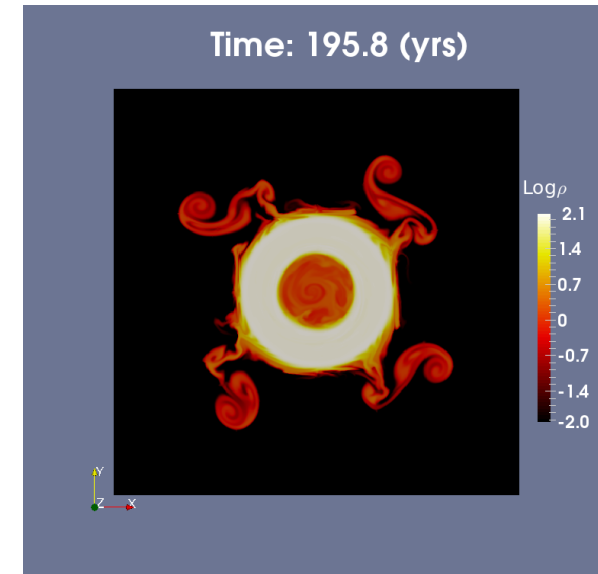
σ



$\sigma = 0.001$



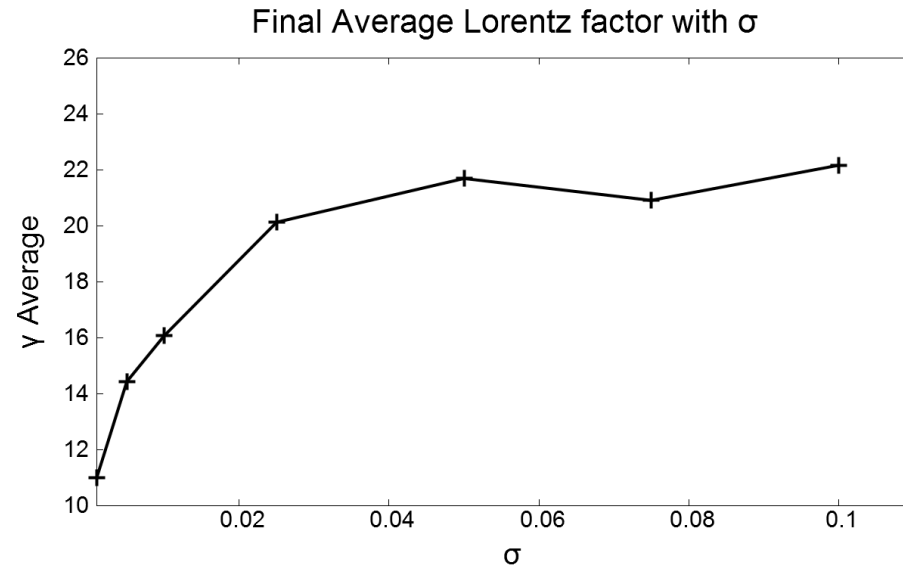
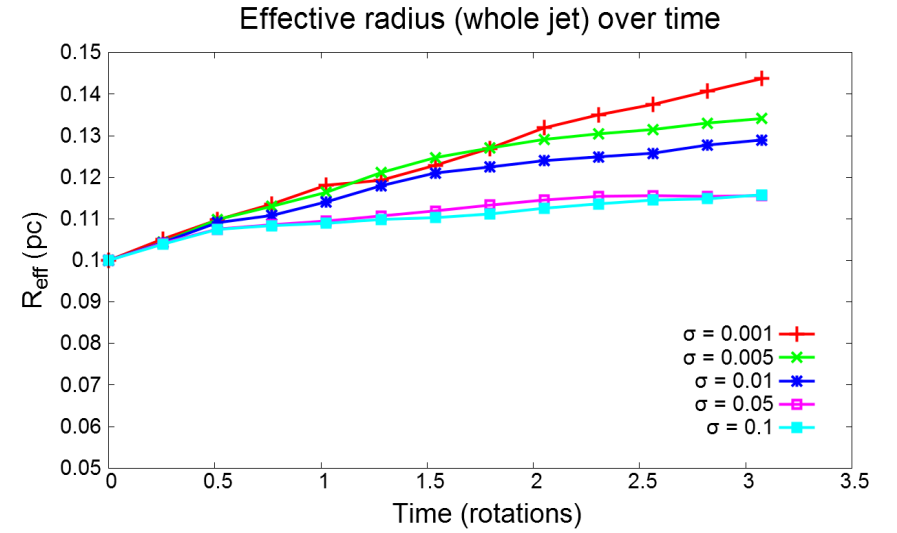
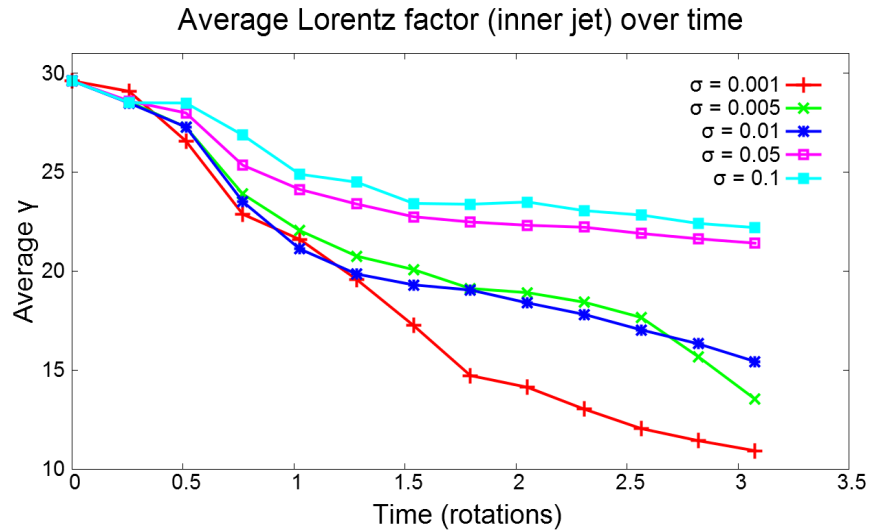
$\sigma = 0.01$



$\sigma = 0.1$

$t = 3$ rotations

Deceleration – de-collimation of the jet



Conclusions

Rotation of relativistic jet induces RT centrifugal instability.

Toroidal magnetic field stabilise the jet against RT instability.